Carbohydrate Polymers 85 (2011) 97–104

Contents lists available at ScienceDirect

Carbohydrate Polymers

journal homepage: www.elsevier.com/locate/carbpol

Preparation and characterization of sorbitol modified nanoclay with high amylose bionanocomposites

Huihua Liu [a], Deeptangshu Chaudhary [a,*], Shin-ichi Yusa [b], Moses O. Tadé [a]

[a] Department of Chemical Engineering, Curtin University of Technology, Perth, Australia
[b] Department of Materials Science and Chemistry, University of Hyogo, Himeji, Japan

ARTICLE INFO

Article history:
Received 11 November 2010
Received in revised form
14 December 2010
Accepted 31 January 2011
Available online 2 March 2011

Keywords:
Starch nanocomposite
Sorbitol
XRD
^{13}C NMR

ABSTRACT

We investigate the influence of sorbitol and natural Na^+-montmorillonite (nanoclay) loading on the characteristic of high amylose nanocomposites and the distribution of nanoclay after extrusion processing. The innovative aspect is the modification of the nanoclay using the sorbitol plasticizer, and as shown in the XRD results, good intercalated/exfoliated morphology had been achieved in all nanocomposites. The expansion of nanoclay gallery relates to sorbitol loading and nanoclay concentration. Evidence of newly formed hydrogen bonds, due to plasticizer and nanoclay interaction, and also the ternary interaction among starch/sorbitol/nanoclay were taken from peaks associated with –OH stretching located at 3300 cm^{-1} and 999 cm^{-1} from the FTIR spectra. Further, ^{13}C NMR spectra demonstrated that the sorbitol mobility was significantly lowered with 1% nanoclay and overall, sorbitol mobility was lower than that of starch chains. TEM directly supported the presence of exfoliated and intercalated/exfoliated morphologies. Furthermore, calorimetric analysis revealed that the glass transition temperature (T_g) decreased with increasing sorbitol content and the presence of nanoclay improved the thermal stability and crystallinity of corresponding samples.

1. Introduction

Biodegradable nanocomposites especially that of polymer obtained from agro resource such as polysaccharides (e.g., starch) have lured enormous interest due to its environmental friendly and competitive properties in mechanical properties, thermal properties, permeability, etc. (Chivrac, Gueguen, Pollet, Ahzi, Makradi & Averous, 2008; Chivrac, Pollet & Avérous, 2009; Chivrac, Pollet, Dole & Avérous, 2010; Cyras, Manfredi, Ton-That & Vázquez, 2008; Zeppa, Gouanv & Espuche, 2009). The most intensive researches are focused on layered silicates, and specially on Na^+-montmorillonite (nanoclay) due to their availability, versatility and low environment and health concerns (Raquez, Nabar, Narayan & Dubois, 2007). Nanoclay is the reinforcing phase due to its very high aspect ratio (100) and due to its low loading requirement (1–10 wt%), and thus different nanocomposite morphologies ranging from intercalated (small amount of polymer moves into the gallery spacing between the silicate platelets), exfoliated (completely and uniformly dispersed in polymer matrix) (Dean, Yu & Wu, 2007; Namazi, Mosadegh & Dadkhah, 2009) and mixed could be produced (Liu, Chaudhary, Yusa & Tadé, 2011; Namazi et al., 2009; Xiong, Tang, Tang & Zou, 2008). A recent study on clay exfoliation process has pointed out that interaction between nanoclay and plasticizer was the dominant factor within the clay exfoliation process (Chivrac et al., 2010). However the modification of clay itself is a tricky process which involves hosts of factors. A key aspect of this work is the modification of the natural nanoclay using the plasticizer (sorbitol) in a single step melting/dissolution process and followed by polymer matrix (high amylose) penetration during dual-melted extrusion.

The objective of the present work was to investigate the combined effect of sorbitol concentration and nanoclay loading in the structural, morphology, thermal properties of prepared nanocomposite. Our efforts are focused on seeking the relationship between the structure, morphology and plasticizer concentration as well as the state of dispersion of the nanoclay within the nanocomposite.

2. Materials and methods

2.1. Materials, nomenclature and processing

Amylose starch (about 70% amylose) was purchased from National Starch Company (New Jersey, USA); sorbitol was obtained from Food Dept Ltd. (Melbourne, Australia); nanoclay (99.5% pure) was supplied by NichePlas Ltd. (Sydney, Australia). 13 samples were prepared at different ratios of nanoclay/sorbitol content. The sam-

* Corresponding author. Tel.: +61 892662522; fax: +61 892662681.
E-mail addresses: Huihua.liu@postgrad.curtin.edu.au (H. Liu), d.chaudhary@curtin.edu.au (D. Chaudhary), yusa@eng.u-hyogo.ac.jp (S.-i. Yusa), M.O.Tade@curtin.edu.au (M.O. Tadé).

0144-8617/$ – see front matter © 2011 Elsevier Ltd. All rights reserved.
doi:10.1016/j.carbpol.2011.01.058

Table 1
Experimental sheet for sample preparation and characterization results (moisture content, *d-spacing*, crystallinity, glass-transition temperature and melting temperature).

Sample ID	Moisture (%) (S.D. = 1%)	*d-spacing* (Å)	Δd (Å)	Xc[a] (%) (S.D. = 2%)	T_g (°C)	T_m (°C)
PS	2.2	–	–	7.48	49.5	128.53
S010	2.71	–	–	5.28	45.73	125.84
S020	2.14	–	–	3.76	25.75	126.04
S105	2.38	Exfoliated	–	4.50	49.6	123.44
S115	4.83	18.044	6.344	3.73	47.5	132.01
S200	6.19	16.532	4.832	8.23	60.17	124.43
S210	3.23	18.189	6.489	4.01	47.73	115.28
S220	4.53	18.044	6.344	6.11	31.25	124.94
S305	3.52	17.544	5.844	7.81	53.4	126.32
S315	2.53	18.179	5.479	4.32	50.4	133.85
S400	5.67	18.116	6.416	12.5	68.95	120.55
S410	2.45	18.572	6.872	8.28	55.5	123.79
S420	2.07	18.638	6.938	6.56	33.83	133.25

Molecular structure[b]

Sorbitol

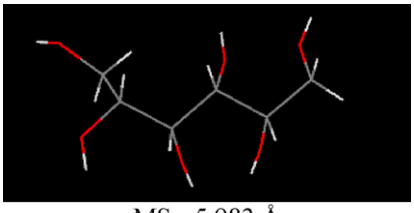

MS_a=5.983 Å

Maltodextrin

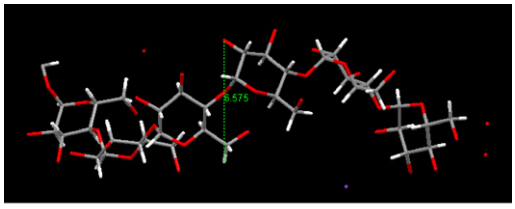

MS_a=6.575 Å

$\Delta d = d_{sample} - d_{pristine\ clay}$.
[a] Crystallinity calculated from the method described in Lopez-Rubio et al. (2008).
[b] Molecular structures are obtained from CCDC; colors: carbon atoms are gray, hydrogen-white, and oxygen-red).

ple nomenclatures used in this work are listed in Table 1. Each sample was described with a label such as S105, where S referred to sorbitol; number 1 indicated 1% nanoclay; the latter two numbers "05" referred to the amount of sorbitol within the samples. Detailed processing parameters and methodology could be found in our previous publication (Liu et al., 2011). Sorbitol was mixed with the MMT nanoclay at known concentrations in excess DI water and this mixture was sonicated for over 2 h to achieve MMT intercalation with sorbitol plasticizer, as shown in Fig. 1(a).

2.2. Characterization studies

Transmission electron microscopy (TEM) was carried out on the samples with nanoclay to determine the extent of nanoclay dispersion. TEM was performed on ultrathin sections at JEM-2100 microscope (JEOL, Tokyo, Japan), operating at an accelerating voltage of 200 kV. Samples were sectioned at room temperature with diamond knife at Leica Ultramicrotome (EM UC7, Tokyo, Japan). Obtained sections were 100 nm in thickness and they were sandwiched between two 400-mesh copper grids for observation.

X-ray diffraction is an important method to quantify the intercalated/exfoliated morphology in nanoclay composites. XRD measurements of the prepared samples were performed in a Bruker Discover 8 diffractometer (Bruker Co., Germany) operating at 40 kV and 40 mA with a 2θ range from 3° to 30° at a scanning rate of 0.5°/s. The basal spacing of the silicate layered was determined from the Bragg's equation, $\lambda = 2d \sin\theta$ (where θ is the diffraction position and λ is the wavelength).

The Fourier transform infrared (FTIR) spectra of all the samples were recorded in PerkinElmer 400 spectrometer (PerkinElmer, USA) using standard accessories in the range of 4000–515 cm^{-1} for 74 scans. The water content in samples was measured by a moisturemeter (CA-100, Mitsubishi, Japan), and the averaged value from three measurements was recorded.

DSC measurement was performed on SEIKO 6200 (Seiko, Japan). About 10 mg sample was placed in an aluminum sealed sample pan.

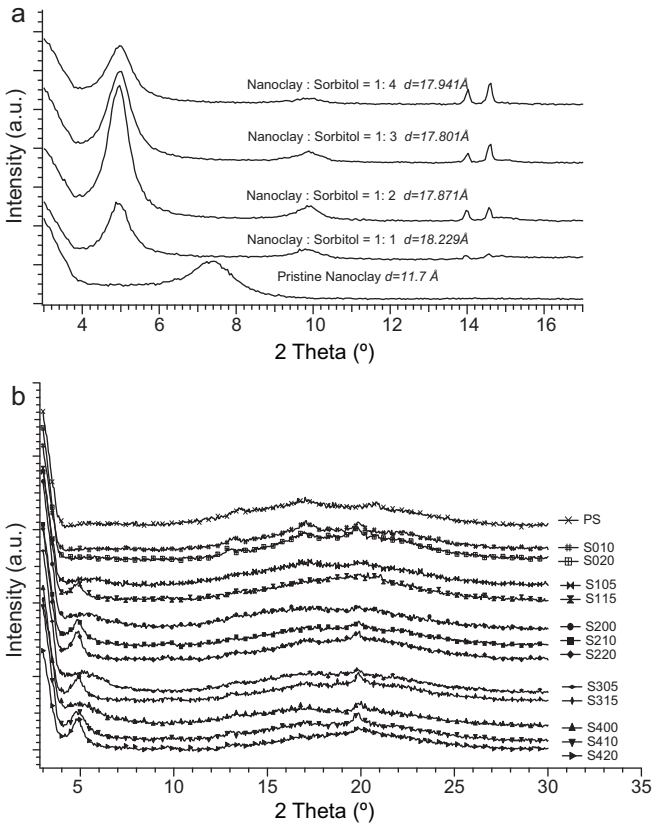

Fig. 1. (a) XRD diffractograms for sorbitol modified nanoclay; offset had been applied for better separation from original overlapped data and (b) XRD diffractograms for sorbitol plasticized nanocomposites.

Samples were heated from −50 °C to 250 °C at a heating rate of 5 °C/min, then kept at 250 °C for 5 min followed by cooling down to 25 °C at 10 °C/min. The glass transition temperature (T_g) was taken as the inflection point of the increment of specific heat capacity. Melting temperature and melting enthalpy were recorded for analysis as well.

Dry powder sample was dissolved in DMSO-d_6, which is accepted to be one of the best solvent for starch-nanocomposite in solution. NMR measurement and the treatment of a nanocomposite with DMSO-d_6 does not affect the structural characteristic (Fournaris, Karakassides, Petridis & Yiannakopoulou, 1999). 0.1 g of powder sample was mixed in 1.5 ml DMSO-d_6 for 10 min and kept in oven for two days at 80 °C to optimizing the solubility of nanocomposite, the samples were hand shaken during the storage period (Schmitz, Dona, Castignolles, Gilbert & Gaborieau, 2008). The ^{13}C NMR spectra were collected at 12,000–20,000 scans (depending on the resolution of spectra obtained) on Bruker 500. The chemical shift scale was calibrated using the residual DMSO-d_6 signal at 39.52 ppm (Hoffman, Arzuan, Pemberton, Aserin & Garti, 2008).

3. Result and discussion

3.1. Morphological analysis

The X-ray diffraction (XRD) pattern, shown in Fig. 1(b), indicated that all nanocomposite samples achieved an increase in the *d-spacing* regardless of the nanoclay content. The *d-spacing* value also suggest that amylose and/or sorbitol molecules migrated into the gallery spacing of nanoclays, and this suggestion is based on the molecule sizes for sorbitol/amylose fragments that reasonably agree with the Δd values (see Table 1). Further analysis can be carried out by dividing all samples into four group based on the nanoclay loading, as shown in Table 1.

It could be read from the XRD plot that *d-spacing* increased with an increase in sorbitol and nanoclay amounts; correspondingly, S420, the sample with highest amount of sorbitol and nanoclay imposed the highest *d-spacing* value of 18.636 Å, Table 1. This is attributed to an overall dominant interaction between the hydrophilic amylose and sorbitol plasticizer, which can facilitate the polymer to penetrate into the hydrophilic nanoclay gallery. This observation differs from our findings with glycerol (a smaller hydrophilic plasticizer) and starch nanocomposites where an increased glycerol content reduced the gallery expansion/exfoliation of nanoclay particle (Liu et al., 2011).

TEM image for representative samples are shown and it is representative of most samples (mixed morphologies). Our processing achieved well intercalated morphologies with a higher 'gallery spacing' in all nanocomposites, Fig. 2. However, a high degree of exfoliation was observed in S105 sample (94%starch/5%sorbitol/1%nanoclay), and this is a likely effect of high polymer and plasticizer to nanoclay ratio, which provides proportionally higher polymer free –OH groups to interact with the nanoclays. It is thought that stabilization of sorbitol in natural nanoclay attracts greater starch chains due to their inherent hydrophilicity and improves polymer/nanoclay interaction during extrusion processing.

From the XRD patterns, it is seen that 5% sorbitol samples have the greatest impact on nanoclay gallery spacing. According to the theory of kinematical scattering, peak broaden is caused by either reduced crystal size or presence of large defects (Ungar, 2004) and the broadened peaks for 5% sorbitol (in S105 and S305) strongly indicate that greater polymer/nanoclay interaction has been achieved by using sorbitol as the modifier for nanoclay. On the other hand, the sharp peaks for higher sorbitol amounts suggested that the stronger polymer/plasticizer interaction became dominant and reduced the amount of nanoclay intercalation. In other words, 5% sorbitol apparently can provide a balance of interactions between greater nanoclay–plasticizer or polymer–plasticizer within a completely hydrophilic system.

3.2. Moisture measurement and crystallinity

Starch equilibrium moisture measurements can indirectly indicate the strength and direction of interaction between the starch–sorbitol and starch–nanoclay. In order to determine the absolute moisture content of prepared samples, samples were oven-dried for 20 h to remove the free water. The results for bound moisture content are shown in Table 1; standard deviations for measurements were within ±1%.

Further, from Fig. 1(b), composites crystallinity could be calculated on the basis of a peak fitting procedures put forward by Rubio et al. (Lopez-Rubio, Flanagan, Gilbert & Gidley, 2008) where they illustrated that this method, widely used for synthetic polymer, was better in reflecting the crystalline content of starch than the traditional two-phase model (Gernat, Radosta, Anger & Damaschun, 1993; Gidley & Bociek, 1988). The method used here took into account irregularities in crystals that were expected to co-exist in semicrystalline materials and avoided the underestimation (two-phase method did not consider the diffuse scattering from non-perfect crystalline structure) of the crystalline content. Igor software package (Wavemetrics, Lake Oswego, Oregon) was used for curve fitting. The fitted coefficients were calculated based on minimized value of Chi-square using the Levenberg–Marquardt algorithm. Each fitting procedure was repeated eight times with different initial inputs to check for data reproducibility. As Rubio et al. (Lopez-Rubio et al., 2008) suggested, Gaussian shape had been confirmed to reflect the best fitting results even with poor initial guess, and the crystallinity for samples is calculated as, $Xc = \sum_1^n ACi/At$, where ACi is the area under each fitted crystalline peak with index i and At is the total area under the diffractogram pattern. The averaged crystallinity results are shown in Table 1, standard deviations for crystallinity calculations are within ±2%.

All extruded samples showed lower crystallinity as compared to that of the native high-amylose starch (crystallinity of around 20%) (Cheetham & Tao, 1998), as shown in Table 1 indicating that the processing technique used here is able to develop a larger amorphous structure, and this is good for applications of thin-film packaging. Also, the nanocomposite crystallinity was dominated by the sorbitol concentration; addition of sorbitol dramatically decreased the crystallinity, e.g., crystallinity decreased from 7.48% (PS) to 5.28% after adding 10% sorbitol to starch polymer. Incorporation of nanoclay led to a higher crystallinity regardless the plasticizer content, and this resulted from the well-known nucleating effect of the nanofiller (Misra, Yuan, Chen & Yang, 2010; Yuan, Chen, Yang & Misra, 2010). Meanwhile the plasticization effect of sorbitol is seen from the decrease of crystallinity with increasing sorbitol concentration for constant nanoclay content (except for 2% nanoclay samples), for example X_C decreased from 8.28% to 6.56% for S410 and S420. This trend was valid for samples with 1% and 3% nanoclay samples, as seen in Table 1.

Addition of sorbitol significantly decreased the equilibrium moisture content; the moisture content for S200 and S210 was 6.19% and 3.23%, respectively. This reduction could be attributed to the strong interaction between sorbitol and starch matrix where water molecules that are present with the polymer structure are replaced by sorbitol molecules. The data shown in Table 1 indicates a complex interaction between the starch, the plasticizer and the nanoclay depending upon their relative concentrations (Chaudhary, 2010; Chaudhary, Adhikari & Kasapis, 2010). Two prominent tendencies were observed based on the moisture content values in Table 1. It is important to remember that moisture

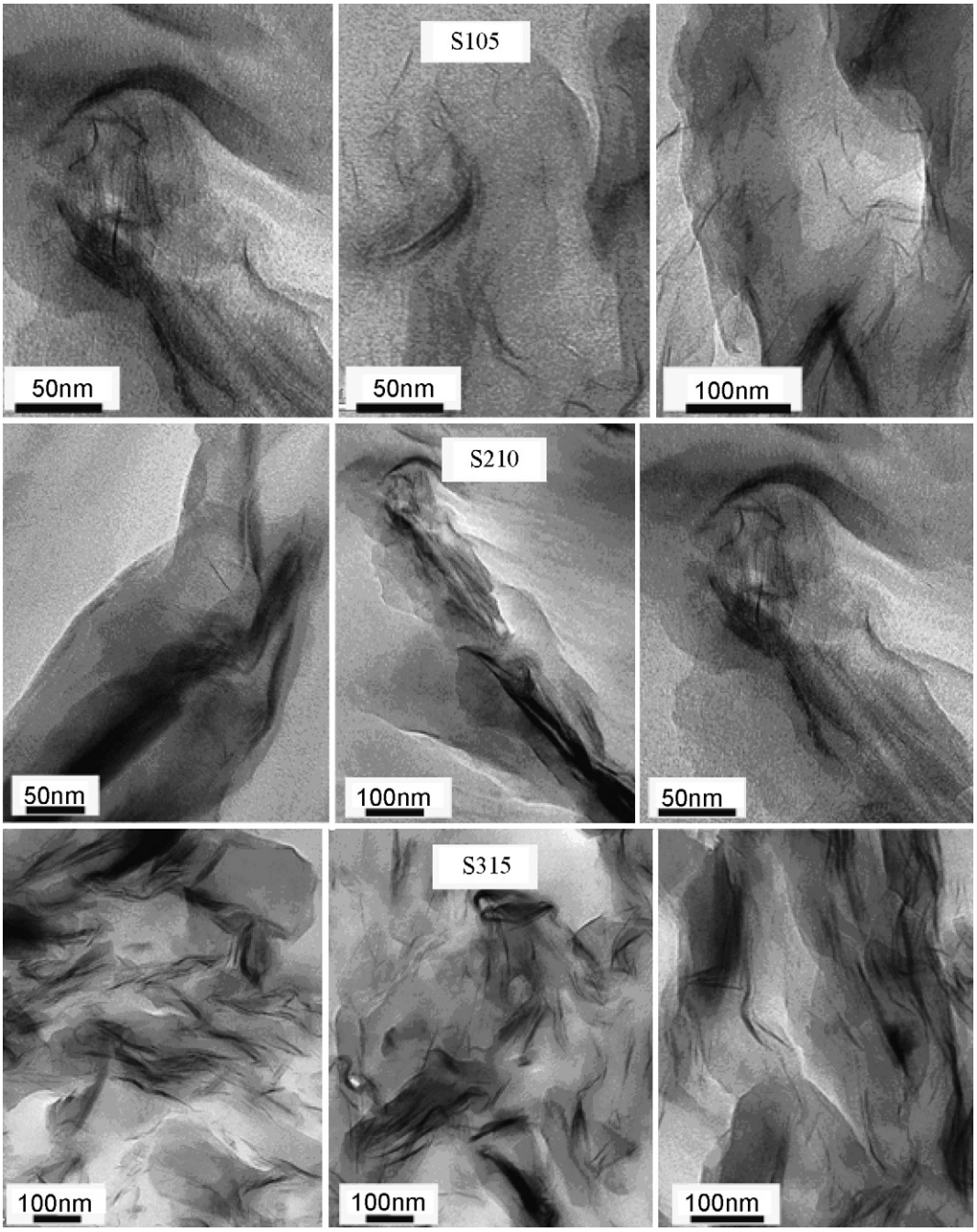

Fig. 2. Representative TEM for sorbitol plasticized nanocomposites.

content varies based on the active –OH sites available in any system. In this system, samples showed higher moisture content for increased sorbitol amount due to the hydrophilic nature of sorbitol molecule. However, as the nanoclay content was increased, greater sorbitol could interact with the nanoclay, and this compounded with relatively stronger starch–sorbitol interaction, decreased the equilibrium moisture content. Interestingly, if sorbitol concentration was fixed, it was found that the equilibrium moisture content was inversely proportional to the nanoclay loading except for S105 and S305. The high moisture content from low nanoclay content samples is believed to be a result of a lower proportion of sorbitol that is involved in the interaction between sorbitol/nanoclay thus relative higher moisture absorbed as a result of sorbitol's typical plasticization effect.

3.3. FTIR results

In Fig. 3, we note typical saccharide bands region located across 1180–953 cm^{-1} which was often considered as the vibration modes of C–C and C–O stretching and the bending mode of C–H bonds. These bands had relatively higher intensities due to their dominance in the make-up of the starch matrix (Mousia, Farhat, Pearson, Chesters & Mitchell, 2001). Also bands at 3300 cm^{-1}, 1630 cm^{-1} and the broader peak centered around 2200 cm^{-1} are typical bands that are associated with individual biopolymer components in addition to the contribution made by the adsorbed water molecules (Souza & Andrade, 2002).

FTIR spectra for starch/nanoclay samples are shown in Fig. 2, and the shift of band 3627 cm^{-1} (from the free OH group of pristine

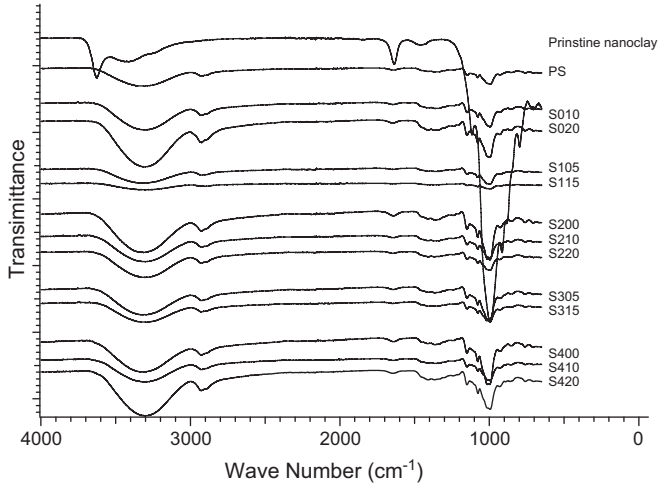

Fig. 3. FTIR spectra for pure starch, pristine nanoclay and nanocomposite; offset had been applied for better separation from original overlapped data.

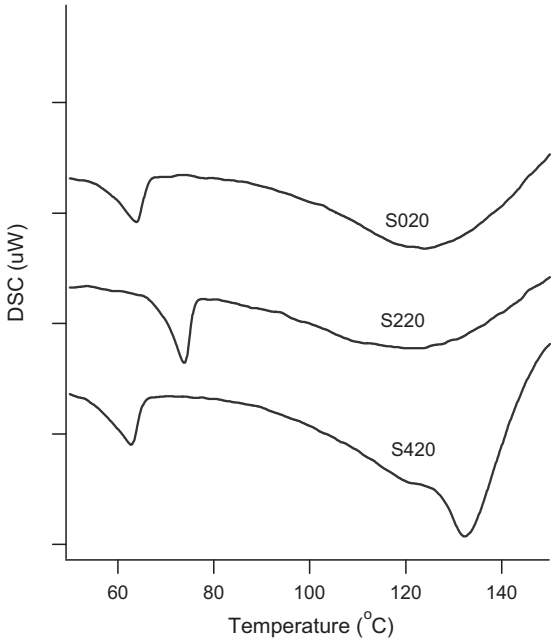

Fig. 4. DSC curves for sample with 20% sorbitol, temperature range from 50 to 150; offset had been applied for better separation from original overlapped data.

nanoclay surface) to a lower frequency, 3302 cm^{-1} clearly indicates the interaction between starch and nanoclay, and similar findings are reported in Field et al.'s work (Field, Sternhell & Kalman, 2002). Comparing the spectrum of pristine nanoclay and spectra from nanocomposites, Fig. 2, the disappearance of the broader peak of H–OH stretching of water around 3234–3486 cm^{-1} indicates the replacement of free water in the interlayer of pristine nanoclay by plasticizer/starch during the processing (Xu, Zhou & Hanna, 2005) and this corroborates the XRD results that the *d-spacing* expands to different extent in all nanocomposite samples. This also suggested that polymer and plasticizer can 'compete' for nanoclay gallery space.

The starch and its nanocomposites present similar peaks in the FTIR spectra regions except the peaks related to –OH stretching at 3290 cm^{-1}, 1630 cm^{-1} and at 1046 cm^{-1}. Comparison based on samples with fixed nanoclay wt% and varying sorbitol showed two bands at higher wavelength that exhibit a peak size that is proportional to sorbitol concentration, Fig. 2. It is important to understand the band changes, mentioned above from 3290 cm^{-1} to 1046 cm^{-1}, associated with –OH groups oscillation modes that are attributed to the formation of new hydrogen bonds and therefore, interactions within the system (García, Ribba, Dufresne, Aranguren & Goyanes, 2009). The presence of new hydrogen bonding (double peaks at 2919–2887 cm^{-1} and 999–992 cm^{-1} in nanocomposite samples when compared with pure starch (Ding, Ainsworth, Plunkett, Tucker & Marson, 2006)) indicated the polymer migration within nanoclay galleries or the polymer wrapping of intercalated nanoclays. The double peak of O–C stretching band at 999–992 cm^{-1} results from bending both 'O' of C–O–H and 'O' of anhydrous glucose ring in starch molecules (Pushpadass, Marx & Hanna, 2008). Therefore, it could be concluded that the developmental work for nanoclay treatment and the processing successfully brought ternary interactions among starch/sorbitol/nanoclay system, and similar findings was reported in our previous article (Liu et al., 2011).

3.4. Differential scanning calorimetry

The DSC thermograms of neat extruded starch, starch/sorbitol composites and starch/sorbitol/nanoclay nanocomposites exhibited glass transitions and crystallite melting endotherm typical of a semi-crystalline polymeric system. The values of T_g and T_m for all samples are presented in Table 1.

Neat extruded sample has a T_g value of 49.5 °C, Table 1, similar to the result reported in Viguié et al.'s work that unplasticized starch had a unique transition around 50 °C (Viguié, Molina-Boisseau & Dufresne, 2007), and T_g value reduced with increased sorbitol concentration in the sample; from 49.5 °C to 45.94 °C and 25.75 °C for 10%(S010) and 20%(S020). This is due to the plasticizing effect that improves the mobility of starch polymer chain. The T_g for nanocomposites increased dramatically from 49.5 °C to 60.17 °C for S200 and 68.95 °C for S400; this was similar to recent reports by Zeppa et al. (2009). Furthermore, the decrease in T_m upon addition of nanoclay was attributed to the reduced crystalline size and presence of crystal imperfections due to physical incompatibility of starch and nanoclay, which suppresses the amylose chains to reorganize and crystallize. However, it should be noted that the presence of nanoclay can allow smaller crystalline fractions to grow due to its nucleating effect and this is manifested in the larger crystallinity degree in XRD measurements (Table 1). The above-mentioned starch–sorbitol interaction and the reduced mobility of the polymer can be further seen in samples with 10% sorbitol which had significantly higher T_g value (from 45.94 °C (S010) to 55.5 °C (S410)), which strongly indicate polymer–plasticizer and polymer–nanoclay interactions.

Increasing the sorbitol content further highlights the typical anti-plasticization to plasticization threshold. The most interesting aspect is the suppression or even disappearance of 'anti-plasticization' behavior of starch–sorbitol composites by the addition of nanoclay and causing an insignificant change in the T_g value (Chaudhary, Adhikari, & Phan, 2009). Anti-plasticization is well known with lower sorbitol concentration because of strong starch–sorbitol interaction that limits starch mobility and increases T_g. Therefore, when comparing samples with 5 wt% sorbitol, increasing the amount of nanoclay (S105 comparing to S305) increased the T_g value from 49.6 °C to 53.4 °C, and this could be explained by considering that the nanoclay was able to 'house' sorbitol and some water molecules such that, one, inter-molecular chain association was prevented by the nanoclay, and second, the interaction between amylose chain and sorbitol was reduced and this hindered the appearance of anti-plasticization effect. Similar

finding was observed in 10% sorbitol samples. The T_g values for S210 and S410 were 47.73 °C and 55.5 °C, respectively.

Two melting endotherms as shown in Fig. 4, and they were observed in high-sorbitol samples which indicate the phase separation within corresponding composite. First T_m is ascribed to be the sorbitol-rich phase and the second T_m to low-sorbitol or nanoclay-rich domain. Such phase separation between domains rich and without nanofillers induced by high plasticizer content of starch formulation could further explain the interesting moisture measurement and crystallinity behavior discussed earlier and similar results have been published by other leading starch biopolymer researchers (Chivrac et al., 2010; Ma, Yu & Wang, 2007).

Table 2
ΔI values for sorbitol/starch/nanoclay composite calculated denoted peaks from ^{13}C NMR spectra.

Sample ID	Sorbitol/starch ratio	S/N value	ΔI
S105	5/94	12.14	0.648
S305	5/92	9.46	1.037
S210	10/88	7.74	1.691
S410	10/86	7.56	1.732
S115	15/84	10.78	2.658
S315	15/82	7.25	3.067
S220	20/78	6.56	2.687
S420	20/76	5.5	2.703

3.5. ^{13}C NMR

During the preparation of NMR samples, nanoclay precipitation was observed; however, a mass balanced indicated that not all nanoclay precipitated, indicating that the morphologies that were exfoliated or even highly intercalated were able to form hybrids within the solutions. NMR studies showed that S/N ratio (define as $S/N = I_{starch\text{-}1}/I_{noise}$) greatly decreased after addition of nanoclay (13.33 and 8.87 for pure starch and S200), Table 2, due to the interaction between nanoclay and starch chains. In other words, starch/nanoclay hybrids are strongly influenced by the clay surface polarity and the clay/matrix interactions. Due to the smaller molec-

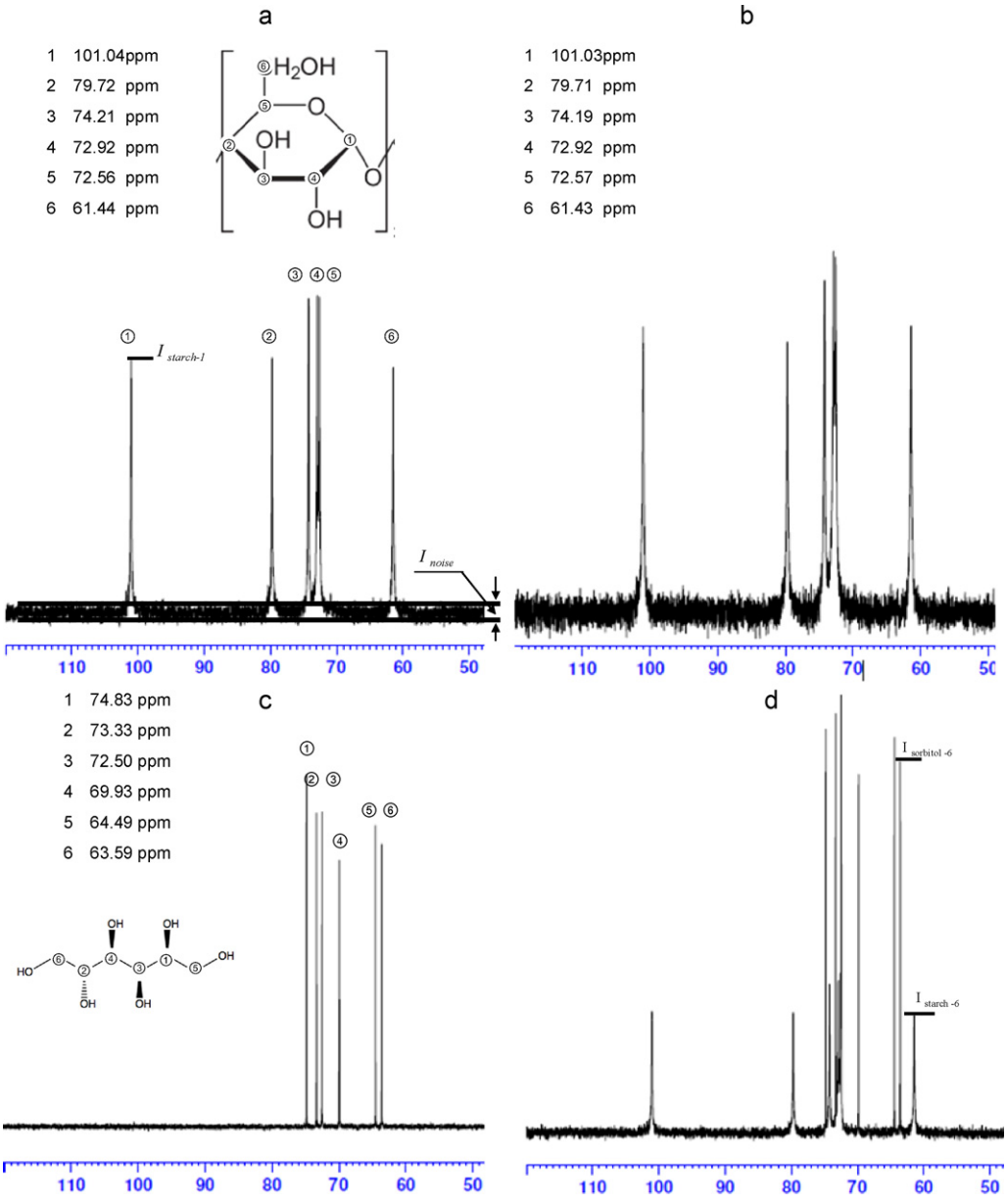

Fig. 5. ^{13}C NMR spectrums for (a) pure starch (b) S200 (c) pure sorbitol and (d) S020.

ular size, the mobility of sorbitol was significantly larger than that of starch chain with in the starch/sorbitol samples, Fig. 5(d). However the relative ratio of sorbitol and starch peaks is dependent on the initial ratio of sorbitol/starch within the nanocomposites. Selecting two well-separate peaks (number 6 for sorbitol and number 6 for starch) from both sorbitol and starch spectrum, Fig. 5(d), denoted as $I_{sorbitol}$ and I_{starch}, the relative ratio of $\Delta I = (I_{sorbitol\text{-}6}/I_{starch\text{-}6})$ was calculated as 6.93 and 4.04 for S020 and S010, respectively. This was obvious because of the higher amount of sorbitol in S020 sample. However, ΔI for S020 was not double the value than that for S010 ($\Delta I_{S020}/\Delta I_{S010} = 1.71$), and the key argument for this behavior is the stronger interaction between starch and sorbitol that 'held' more sorbitol within the starch network and restricted the movement of sorbitol.

Table 2 also shows that the *S*/*N* ratio was overall lower for samples with nanoclay than that from samples without nanoparticles. This is typical of nanocomposite samples that result in a lower spectra resolution, for example the *S*/*N* values are 7.25 and 5.5 for S020 and S420, respectively. Decrease in *S*/*N* value and broadening of peaks for nanocomposites spectra indicate the interactions of nanoclay/sorbitol/starch. The reduction in spectral resolution was also attributed to reduced mobility of the sorbitol/starch by nanoclay platelets, and further corroborated the impact of processing conditions in developing high homogeneity nanocomposites from completely hydrophilic systems. As read from Table 2, ΔI values increasing upon the sorbitol amount (except S105) regardless the nanoclay concentration which was attributed to larger proportion of high mobility sorbitol molecules. Also, increasing the nanoclay at fixed sorbitol concentration resulted in higher ΔI value due to stronger interaction between starch chains and nanoclay that influenced the sample concentration; however the highest ΔI values came from S315 rather than S420.

A different behavior was observed where the signal peak from sorbitol were lower than that from starch chain (ΔI value for S105 is lower than 1) which meant that in S105, the mobility of sorbitol was unexpectedly lower than that of the long chain starch. This behavior might be linked to the argument that lower sorbitol concentrations could separate the starch/sorbitol and nanoclay/sorbitol interactions without competing with other interactions, and such argument had been put forward in our previously report (Liu et al., 2011) and also by Chivrac et al. (2010) when they investigated sorbitol and other plasticizers for nanoclay/starch interactions. Thus, incrementing sorbitol or nanoclay (S115 or S305) translated binary interactions (sorbitol/starch, sorbitol/nanoclay and nanoclay/starch) into ternary interactions that could result in a competition within a more saturated/ordered network, thus leading to a higher ΔI value. Such hypothesis could be corroborated by the XRD result where S105 exhibited exfoliated morphology rather than intercalated structure, whereas the other samples exhibited predominantly intercalated morphologies, Fig. 1(b).

4. Conclusion

The influence of ratio of sorbitol/nanoclay, varied from 1% to 20% for sorbitol (at interval of 5%) and 1 to 4% for nanoclay, on the characteristic of extruded starch nanocomposites was studied in the present work. XRD results confirmed the expansion of *d-spacing*, to different extent depended on the sample formulation. Higher degree exfoliation morphology was observed in S105 and nanoclay *d-spacing* increased with increasing sorbitol concentration. FTIR measurements concluded the presence of interactions between starch biopolymer and nanoclay (with sorbitol) from the shift of band 3627 cm^{-1} (free –OH group on nanoclay) to a lower frequency 3302 cm^{-1}. The double peak at 2919–2887 cm^{-1} and 999–992 cm^{-1} in extruded composite samples was compared with native starch and this shift confirmed the newly formed hydrogen bonding.

DSC had been carried out to determine the thermal properties of prepared samples. Addition of nanoclay did dramatically increase the T_g for samples without sorbitol. Nanoclay concentration turned out to be the main factor that increased the T_g in nanocomposites sample which might due to the high T_g for pristine nanoclay. Nanoclay was also successful in balancing the starch–sorbitol interaction to limit anti-plasticization. *S*/*N* greatly decreased after addition of nanoclay, due to the interaction happened between nanoclay and starch chains resulted in the decrease of concentration in the prepared sample in ^{13}C NMR measurements. ΔI values increasing upon the sorbitol amount (except S105) regardless the nanoclay concentration. Also, bionanocomposite systems where nanoclay or sorbitol was *not limiting*, increasing the nanoclay within samples containing same amount of sorbitol resulted in higher ΔI value; however the highest ΔI values came from S315 rather than S420 and this highlighted the complex ternary interactions within the starch bionanocomposite system.

Acknowledgments

The authors wish to thank Dr. Kyuya Nakagawa for his excellent technical assistance with the DSC measurements. Acknowledge the internal funding from Curtin University of Technology. There is no potential conflict of interest between the researchers and this investigation does not bias any other investigation.

References

Chaudhary, D., Adhikari, B., & Phan, C. (2009). Glass rubber transition of plasticised starch biopolymer affected by relative humidity. *International Journal of Polymers and Technologies*, *1*(2), 101–106.
Chaudhary, D. S. (2010). Competitive plasticization in ternary plasticized starch biopolymer system. *Journal of Applied Polymer Science*, *118*(1), 486–495.
Chaudhary, D. S., Adhikari, B. P., & Kasapis, S. (2010). Glass transition behaviour of plasticized starch biopolymer system-a modified Gordon–Taylor approach. *Food Hydrocolloids*, *25*(1), 114–121.
Cheetham, N. W. H., & Tao, L. (1998). Variation in crystalline type with amylose content in maize starch granules: An X-ray powder diffraction study. *Carbohydrate Polymers*, *36*(4), 277–284.
Chivrac, F., Gueguen, O., Pollet, E., Ahzi, S., Makradi, A., & Averous, L. (2008). Micromechanical modeling and characterization of the effective properties in starch-based nano-biocomposites. *Acta Biomaterialia*, *4*(6), 1707–1714.
Chivrac, F., Pollet, E., & Avérous, L. (2009). Progress in nano-biocomposites based on polysaccharides and nanoclays. *Materials Science and Engineering: R: Reports*, *67*(1), 1–17.
Chivrac, F., Pollet, E., Dole, P., & Avérous, L. (2010). Starch-based nano-biocomposites: Plasticizer impact on the montmorillonite exfoliation process. *Carbohydrate Polymers*, *79*(4), 941–947.
Cyras, V. P., Manfredi, L. B., Ton-That, M. T., & Vázquez, A. (2008). Physical and mechanical properties of thermoplastic starch/montmorillonite nanocomposite films. *Carbohydrate Polymers*, *73*(1), 55–63.
Dean, K., Yu, L., & Wu, D. Y. (2007). Preparation and characterization of melt-extruded thermoplastic starch/clay nanocomposites. *Composites Science and Technology*, *67*(3–4), 413–421.
Ding, Q. B., Ainsworth, P., Plunkett, A., Tucker, G., & Marson, H. (2006). The effect of extrusion conditions on the functional and physical properties of wheat-based expanded snacks. *Journal of Food Engineering*, *73*(2), 142–148.
Field, L. D., Sternhell, S., & Kalman, J. R. (2002). Organic structures from spectra. *Journal of Chemical Education*, *79*(11).
Fournaris, K. G., Karakassides, M. A., Petridis, D., & Yiannakopoulou, K. (1999). Clay-polyvinylpyridine nanocomposites. *Chemistry of Materials*, *11*(9), 2372–2381.
García, N. L., Ribba, L., Dufresne, A., Aranguren, M. I., & Goyanes, S. (2009). Physico-mechanical properties of biodegradable starch nanocomposites. *Macromolecular Materials and Engineering*, *294*(3), 169–177.
Gernat, C., Radosta, S., Anger, H., & Damaschun, G. (1993). Crystalline parts of three different conformations detected in native and enzymatically degraded starches. *Starch-Stärke*, *45*(9), 309–314.
Gidley, M. J., & Bociek, S. M. (1988). Carbon-13 CP/MAS NMR studies of amylose inclusion complexes, cyclodextrins, and the amorphous phase of starch granules: Relationships between glycosidic linkage conformation and solid-state carbon-13 chemical shifts. *Journal of the American Chemical Society*, *110*(12), 3820–3829.
Hoffman, R. E., Arzuan, H., Pemberton, C., Aserin, A., & Garti, N. (2008). High-resolution NMR. *Journal of Magnetic Resonance*, *194*(2), 295–299.

Liu, H., Chaudhary, D., Yusa, S.-I., & Tadé, M. O. (2011). Glycerol/starch/Na+-montmorillonite nanocomposites: A XRD, FTIR, DSC and ^{1}H NMR study. *Carbohydrate Polymers*, *83*(4), 1591–1597.

Lopez-Rubio, A., Flanagan, B. M., Gilbert, E. P., & Gidley, M. J. (2008). A novel approach for calculating starch crystallinity and its correlation with double helix content: A combined XRD and NMR study. *Biopolymers*, *89*(9), 761–768.

Ma, X., Yu, J., & Wang, N. (2007). Production of thermoplastic starch/MMT sorbitol nanocomposites by dual melt extrusion processing. *Macromolecular Materials and Engineering*, *292*(6), 723–728.

Misra, R. D. K., Yuan, Q., Chen, J., & Yang, Y. (2010). Hierarchical structures and phase nucleation and growth during pressure-induced crystallization of polypropylene containing dispersion of nanoclay: The impact on physical and mechanical properties. *Materials Science and Engineering: A*, *527*(9), 2163–2181.

Mousia, Z., Farhat, I. A., Pearson, M., Chesters, M. A., & Mitchell, J. R. (2001). FTIR microspectroscopy study of composition fluctuations in extruded amylopectin–gelatin blends. *Biopolymers*, *62*(4), 208–218.

Namazi, H., Mosadegh, M., & Dadkhah, A. (2009). New intercalated layer silicate nanocomposites based on synthesized starch-g-PCL prepared via solution intercalation and in situ polymerization methods: As a comparative study. *Carbohydrate Polymers*, *75*(4), 665–669.

Pushpadass, H. A., Marx, D. B., & Hanna, M. A. (2008). Effects of extrusion temperature and plasticizers on the physical and functional properties of starch films. *Starch-Stärke*, *60*(10), 527–538.

Raquez, J., Nabar, Y., Narayan, R., & Dubois, P. (2007). New developments in biodegradable starch-based nanocomposites. *International Polymer Processing*, *22*(5), 463.

Schmitz, S., Dona, A. C., Castignolles, P., Gilbert, R. G., & Gaborieau, M. (2008). Assessment of the extent of starch dissolution in dimethyl sulfoxide by ^{1}H NMR spectroscopy. *Macromolecular Bioscience*, *9*(5), 506–514.

Souza, R. C. R., & Andrade, C. T. (2002). Investigation of the gelatinization and extrusion processes of corn starch. *Advances in Polymer Technology*, *21*(1), 17–24.

Ungar, T. (2004). Microstructural parameters from X-ray diffraction peak broadening. *Scripta Materialia*, *51*(8), 777–781.

Viguié, J., Molina-Boisseau, S., & Dufresne, A. (2007). Processing and characterization of waxy maize starch films plasticized by sorbitol and reinforced with starch nanocrystals. *Macromolecular Bioscience*, *7*(11), 1206–1216.

Xiong, H. G., Tang, S. W., Tang, H. L., & Zou, P. (2008). The structure and properties of a starch-based biodegradable film. *Carbohydrate Polymers*, *71*(2), 263–268.

Xu, Y., Zhou, J., & Hanna, M. A. (2005). Melt-intercalated starch acetate nanocomposite foams as affected by type of organoclay 1. *Cereal Chemistry*, *82*(1), 105–110.

Yuan, Q., Chen, J., Yang, Y., & Misra, R. D. K. (2010). Nanoparticle interface driven microstructural evolution and crystalline phases of polypropylene: The effect of nanoclay content on structure and physical properties. *Materials Science and Engineering: A*, *527*(21–22), 6002–6011.

Zeppa, C., Gouanv, F., & Espuche, E. (2009). Effect of a plasticizer on the structure of biodegradable starch/clay nanocomposites: Thermal, water-sorption, and oxygen-barrier properties. *Journal of Applied Polymer Science*, *112*(4), 2044–2056.